


Research Article

Model-Based Control with Active Disturbance Rejection Algorithm for a Diesel Engine

Shun-Liang Ding ¹, Shuai-Feng He,¹ Bi-Qing Tu,² Jin-Jin Liu,¹ Yu-Yuan Wang,³ and En-Zhe Song³

¹School of Mechanical and Power Engineering, Zhengzhou University, Zhengzhou 450001, China

²CSSC Marine Power Zhenjiang Co., Ltd., Zhenjiang 212000, China

³College of Power and Energy Engineering, Harbin Engineering University, Harbin 150001, China

Correspondence should be addressed to Shun-Liang Ding; dingshunliang@126.com

Received 5 August 2022; Revised 13 November 2022; Accepted 26 November 2022; Published 3 January 2023

Academic Editor: Chih-Chiang Chen

Copyright © 2023 Shun-Liang Ding et al. This is an open access article distributed under the Creative Commons Attribution License, which permits unrestricted use, distribution, and reproduction in any medium, provided the original work is properly cited.

To improve the speed control performance of a diesel engine, the active disturbance rejection controller (ADRC) is designed by adding an arranging transition process to the traditional PID controller, extracting differential signals reasonably, and adopting nonlinear combination process to error signals. The ADRC is composed of a tracking differentiator (TD), an extended state observer (ESO), and a nonlinear state error feedback (NLSEF). Such constructed ADRC can adapt to the strong nonlinear and complicate working conditions of diesel engine for power generation. A simulation model of the diesel engine is built to verify the proposed ADRC, and simulation results are in good accordance with the experimental results. To further validate the advantages of the designed ADRC, the traditional PID is improved by TD. Meanwhile, performance comparisons are carried out between traditional PID controller, improved PID controller, and ADRC. Results present that the improved PID controller can achieve a better control performance than that of the traditional PID controller both in steady state and transient state. However, the ADRC can further improve the speed control performance evidently on the basis of the improved PID controller.

1. Introduction

Diesel engine is a complex power machine with high nonlinearity and time-varying characteristics [1], and it often operates under complex conditions such as variable speed, variable load, and variable environment, leading to continuous changes in the operating parameters and serious instability of diesel engine [2]. To ensure the proper operation of diesel engine under complex conditions, the control parameters must be adjusted quickly according to the engine operating status [3]. Moreover, speed control technology is the basic and utmost important technology of diesel engine for power generation [3, 4]. In the basic control strategy of electronic governor, the fuel supply is adjusted automatically according to the external load conditions of diesel engine, so the engine speed can be controlled within a certain range. The PID controller, whose core idea is to minimize error by

error, is commonly used to control the speed of diesel engine and many other industrial machines due to its simplicity and reliability [5–8]. However, with the increasing requirements of control performance, the disadvantages of traditional PID controller disclose gradually [8]. The disadvantages of traditional PID controller are shown as follows: (1) its control performance is not that satisfying when nonlinear, time-varying and disturbance factors are included in the controlled object [8, 9]. Also, diesel engine is a complex machine with fast time-varying, strong disturbance, and strong nonlinearity. It is a challenge to achieve good speed control performance under all operation conditions for diesel engine with traditional PID controller [10]; (2) it is hard to take control performance of both steady state and transient state into consideration [11]. And it is also difficult to deal with nonlinear problems for traditional PID controller because it is constructed of linear deviation combination; (3) the

control parameters are unable to be changed timely according to the change of engine operating status. A large amount of calibration experiments are needed to calibrate the PID control parameters. So the control performance will be greatly affected by the PID control parameters. Thus, small disturbance in engine can lead to great impact on its control performance.

Because of the abovementioned deficiencies, traditional PID controller cannot meet the daily increasing requirements on control performance for engine. New controller or improvement on traditional PID controller is urgently needed. Considering the fact that PID control technology has the advantage of not relying on accurate mathematical model of the controlled object, there is still a large market for optimization and improvement of traditional PID control technology in engineering [11, 12].

With the development of modern control theory, previous researchers tried to combine PID with advanced control algorithms to overcome the abovementioned deficiencies of traditional PID controller and achieve better control performance for diesel engine. These applications included fuzzy-PID controller, genetic-PID controller, NN-PID controller, and so on [13, 14]. As shown in Figure 1, fuzzy-PID controller designed by Xiong et al. [15], whose PID parameters were adjusted by fuzzy logic to improve control performance, was applied on engine speed control. However, the settings of the fuzzy rules may run into rule explosion with increasing control dimension and depend too much on actual experience of the designer.

Optimizing all feasible solutions is the core idea of genetic-PID algorithm. The optimization process of genetic algorithm, which refers to the principle that species in biology mutate during their evolutionary process, can improve its adaptive ability to the external environment. As shown in Figure 2, the three parameters of PID controller are optimized by system identification and genetic algorithm calculation [16, 17], and the optimization process of genetic algorithm is conducted offline according to the system condition. Genetic algorithm is capable of searching for the global optimal parameters, but it is difficult to search for local optimal parameters. Therefore, the genetic algorithm has low efficiency and low convergence speed [18].

NN-PID is a combination of PID and neural network (NN) [19, 20]. As shown in Figure 3, by taking the self-study ability, calculation feed forward, and deviation back-propagation of NN, the system error can be minimized through continuous iterations, and the proper PID control parameters are obtained. Therefore, ideal control performance is achieved by the interaction and intercorrection of NN and PID [21, 22]. However, NN has the disadvantages of large calculation and low convergence speed, and it is hard to meet the real-time requirements of online learning. Therefore, its practical application still has technical difficulties to overcome.

The goal of diesel engine speed control is to achieve a small speed fluctuation under steady-state conditions and a quick speed recovery under transient-state conditions. When the engine is affected by load disturbance or sudden change, the actual overshoot of the transient speed should be

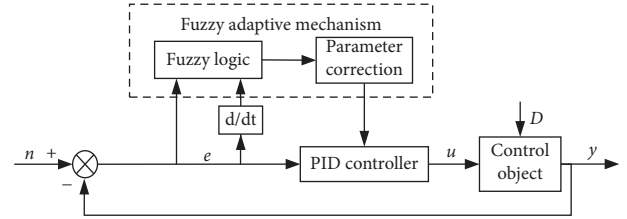


FIGURE 1: Principle of the fuzzy-PID controller.

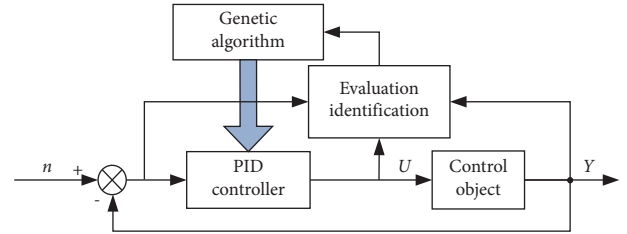


FIGURE 2: Principle of the genetic-PID controller.

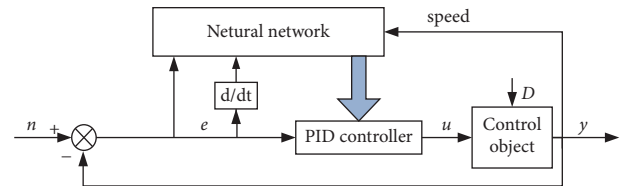


FIGURE 3: Principle of the NN-PID controller.

as small as possible, and the transient speed should also quickly track the target speed. Although the combination of advanced control algorithms and traditional PID can improve the control performance of the system to a certain extent, it does have the disadvantages such as depending too much on actual experience, low efficiency, low convergence speed, and large calculation. Therefore, it is difficult to achieve the optimal control goal of the system, and the idea of only using advanced algorithms to completely and timely adjust the control parameters of traditional PID without improving the controller structure is unable to solve the abovementioned problems.

The speed control of diesel engine needs to consider the nonlinearity, time-varying, model parameter uncertainty, and external disturbance uncertainty of the system. Therefore, besides the direct combination of advanced control algorithms and traditional PID such as fuzzy-PID, genetic-PID, and NN-PID, some researchers also improved the controller structure by using advanced control strategies such as sliding mode control and model predictive control. Sliding mode control, also known as variable structure control, is developed on the basis of phase plane theory. It is a nonlinear control method with the characteristics of fast response speed and strong robustness to external noise interference, overcoming the disadvantage of system uncertainty. Therefore, it has been applied to the diesel engine speed control by some researchers [3, 11, 12]. However, this method depends on accurate mathematical model of the

controlled object, so its application space is limited compared with PID control technology. It should be noted that the diesel engine is a complex nonlinear system, and it is difficult to establish an accurate mathematical engine model, which seriously limits the application of sliding mode control in engine speed control field [23]. The research studies of model predictive control in diesel engine speed control also have some achievements [1]. However, the structure and hardware of model predictive controller are complex, so it is expensive and difficult to be applied in engineering. Furthermore, the external disturbance of the diesel engine cannot be modeled at all. This is another important reason that hinders the engineering application of model predictive control in diesel engine speed control field.

According to the analysis of the above mentioned control methods and the needs of practical engineering application, it is necessary to find a control method that is high real-time and independent of accurate mathematical model of the controlled object. ADRC technology put forward by Han in 1995 [24] is a new control method that combines the advantages of PID control principle and modern control theory [25]. The basic idea of ADRC is “restrain disturbance by disturbance” (i.e., absolute invariance principle and intima principle), rather than direct measurement or preobtained disturbance model. Because of its strong robustness, high reliability, and excellent transient response characteristics, ADRC is applied to deal with linear, nonlinear, time-varying, and time-unvarying problems. Previous research studies on ADRC mainly focused on two aspects. On the one hand, the structure of ADRC was studied for different specific problems. The core components of ADRC are TD, ESO, and NLSEF, in which each component can be collocated arbitrarily, and each component can adjust its structure appropriately. The features of arbitrary combination can produce hundreds of ADRCs with different structures. Furthermore, for a specific problem, a more complex structure does not mean a better control performance. So one of the research hotspots is searching for a proper ADRC structure for different controlled objects, such as decoupling control [26], speed sensor less control, and multimotor synchronous control [27]. On the other hand, ADRC was combined with advanced control algorithms, including sliding mode variable structure control algorithm [28], fuzzy control algorithm [29], neural network, and swarm intelligence algorithm [30], to achieve better control performance. In recent years, ADRC has been widely used in new energy power generation, jet engine control, robot control, and so on. However, it has not been applied in the field of diesel engine speed control [31, 32].

Based on the advantages of ADRC and the disadvantages of other control algorithms mentioned above, the structure of ADRC is studied for the specific problem of the diesel engine speed control. And the ADRC for the engine speed control system is proposed and designed in this paper. Meanwhile, its feasibility is verified by simulations and experiments. This paper is organized as follows: In Section 2, the ADRC is proposed for speed control, and the improved PID controller is also designed with the purpose of comparison. In Section 3, the control-

used simulation model of the diesel engine is given, following with the introduction of engine experimental bench in Section 4. Finally, the comparative simulations and experiments for the different controllers are exhibited in Section 5, proving the reliability and accuracy of the proposed ADRC in the field of diesel engine speed control.

2. ADRC Design

2.1. Principle of ADRC. The theory of ADRC is derived from conventional PID control technology, but the structure of conventional PID is improved by combining the modern control theory. The improvement scheme is as follows:

2.1.1. Transition Process Adjustment. PID controller obtains control parameters through the deviation between the target value and the output of the controlled object, which is not reasonable for nonlinear system. During the control process, the setting of the target value may change suddenly while the output is inertial. It is very difficult to let a gradual change parameter track a sudden change target value, so the reasonable transition process is adjusted according to the target value and the characteristics of the controlled object. Differential signal during the transition process is also provided. The principle of “adding transition process” is illustrated in Figure 4.

In Figure 4, $v(t)$ is the control target, $v_1(t)$ is the transition process according to $v(t)$, and $v_2(t)$ is the differential signal of $v_1(t)$. \sum is a transient process or a function, which can be designed according to $v(t)$ and the characteristics of the controlled object.

2.1.2. Differential Signal Extraction. In the field of control engineering, the differentiator is difficult to be realized in practice and can only be approximated. The transfer function of approximate differentiator commonly used in engineering is $y = (s/(\tau s + 1))v$. This transfer function can be extended to $y = (1/\tau)(1 - (1/(\tau s + 1)))v$ and is a realization of the approximate differential formula $y = ((v(t) - v(t - \tau))/\tau)$. But when the input signal $v(t)$ is affected by noise $n(t)$, the approximate derivative $((v(t) - v(t - \tau))/\tau)$ of the output will be covered by the enlarged noise $(n(t)/\tau)$, leading to unsatisfying control results. Moreover, with the change of external load, the actual engine speed control system will inevitably be affected by noise, so it is necessary to improve the extraction process of differential signal. By applying the approximate formula $y = ((v(t - \tau_1) - v(t - \tau_2))/(\tau_2 - \tau_1))$ to extract the differential signal, the approximate differential value can be obtained through the transfer function (shown in equation (1)), namely, the second-order dynamic segment.

$$y(t) = \frac{1}{\tau_2 - \tau_1} \left(\frac{1}{\tau_1 s + 1} - \frac{1}{\tau_2 s + 1} \right) v(t). \quad (1)$$

Obtaining differential values needs to quickly track the system input, so the following nonlinear TD is generated.

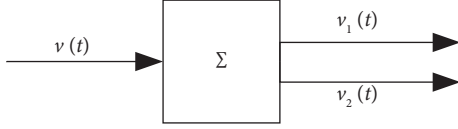


FIGURE 4: Principle of the “adding transition process.”

The fastest closed-loop feedback control system of the second-order integrator is shown in equation (2). The signal $v(t)$ is input according to equation (3).

$$\begin{cases} \dot{x}_1(t) = x_2(t), \\ \dot{x}_2(t) = -r \operatorname{sign}\left(x_1(t) + \frac{x_2(t)|x_2(t)|}{2r}\right), \end{cases} \quad (2)$$

$$\begin{cases} \dot{x}_1 = x_2(t), \\ \dot{x}_2 = -r \operatorname{sign}\left(x_1(t) - v(t) + \frac{x_2(t)|x_2(t)|}{2r}\right), \end{cases} \quad (3)$$

where $x_1(t)$ is used to track the change of the input signal $v(t)$ at the effect of r . $x_2(t)$ as the differential of $x_1(t)$ can be used as the differential of $v(t)$. Because of the Bang-Bang characteristics of the function $-r \operatorname{sign}(x_1(t) - v(t) + (x_2(t)|x_2(t)|/2r))$, tremor is inevitable in steady state. To avoid tremor, the following system shown in equation (4) is introduced to deal with function $\operatorname{fhan}(x_1, x_2, r, h)$ shown in equation (5).

$$\begin{cases} x_1(k+1) = x_1(k) + hx_2(k), \\ x_2(k+1) = x_2(k) - ru(k), \quad |u(k)| \leq r, \end{cases} \quad (4)$$

$$\begin{cases} d = rh^2, \\ a_0 = hx_2, \\ y = x_1 + a_0, \\ a_1 = \sqrt{d(d + 8|y|)}, \\ a_2 = a_0 + \frac{\operatorname{sign}(y)(a_1 - d)}{2}, \\ s_y = \frac{(\operatorname{sign}(y + d) - \operatorname{sign}(y - d))}{2}, \\ a = (a_0 + y - a_2)s_y + a_2, \\ s_a = \frac{(\operatorname{sign}(a + d) - \operatorname{sign}(a - d))}{2}, \\ \operatorname{fhan} = -r\left(\frac{a}{d} - \operatorname{sign}(a)\right)s_a - r \operatorname{sign}(a). \end{cases} \quad (5)$$

Then the differentiator can be defined as follows according to

$$\begin{cases} fh = \operatorname{fhan}(x_1(k) - v(k), x_2(k), r, h), \\ x_1(k+1) = x_1(k) + hx_2(k), \\ x_2(k+1) = x_2(k) + hfh. \end{cases} \quad (6)$$

To preliminarily verify the performance of the differentiator, the system parameters $v = 1$ and $r = 1$ are selected. It can be seen from the simulation results in Figure 5 that x_1 can track the system input $v(t)$ without overshoot, and x_2 is the obtained differential signal.

The TD of v can be described as the sketch map in Figure 6. And the TD is used to track the time-varying signal $v = \sin(t)$ ($r = 50$). It can be seen from the simulation results shown in Figure 7 that the tracking and differential effects are very proper.

2.1.3. Nonlinear Combination. Based on the results of the transition process adjustment by TD, the error of the transition process is obtained as $e_1 = v_1 - x_1$, and the differential signal is obtained as $e_2 = v_2 - x_2$. Thus, the error integral signal can be calculated by $e_0 = \int_0^t e_1(\tau) d\tau$, and the PID control can be achieved by

$$u = k_0 e_0 + k_1 e_1 + k_2 e_2. \quad (7)$$

However, this simple linear combination is unable to achieve the best control performance for complex nonlinear control systems. Thus, an improved PID by introducing nonlinear parts during the control process is necessary. The nonlinear combination method is shown in

$$u = k_0 \operatorname{fal}(e_0, a_0, \delta) + k_1 \operatorname{fal}(e_1, a_1, \delta) + k_2 \operatorname{fal}(e_2, a_2, \delta), \quad (8)$$

$$u = k_0 e_0 + \operatorname{fhan}(e_1, c * e_2, r, h_0), \quad (9)$$

$$\operatorname{fal}(x, a, \delta) = \begin{cases} \frac{x}{\delta^{(1-a)}}, & |x| \leq \delta, \\ \operatorname{sign}(x)|x|^a, & |x| > \delta. \end{cases} \quad (10)$$

The $\operatorname{fhan}(x_1, x_2, r, h_0)$ has already described in equation (5). Unlike the previous equations, the parameter c^* (damping factor) is added to the deviation feedback and the original precision factor h is replaced by h_0 (filter factor for TD filtering).

The parameter a_i in equation (8) should be limited in the proper range shown in equation (11).

$$a_0 < 0 < a_1 < 1 < a_2. \quad (11)$$

Based on the abovementioned improvements, the improved PID structure is shown in Figure 8. In specific application, if the target value does not change so violently, the TD can be used to replace the transition process to simplify the controller structure.

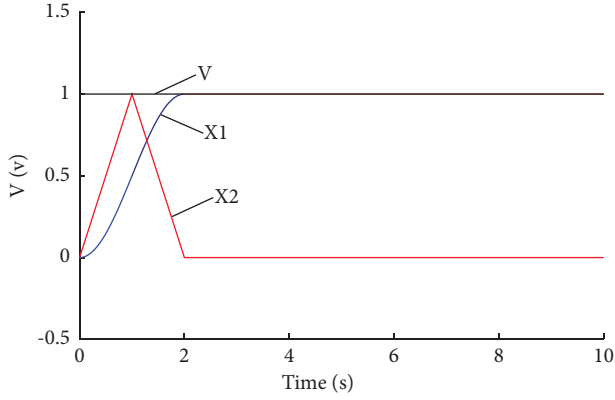


FIGURE 5: Characteristics of the differentiator.

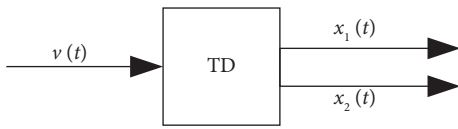
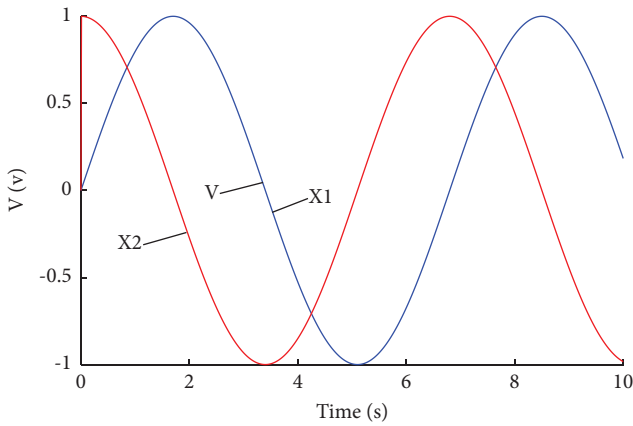
FIGURE 6: Sketch map of the TD of v .

FIGURE 7: Tracking and differential effects of the TD.

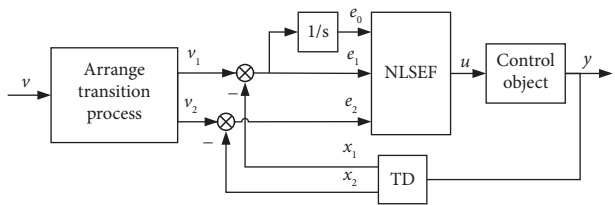


FIGURE 8: Principle of the improved PID controller.

One point should be noted that this improved PID controller can adopt different types of modules according to different systems, such as different “transition process” modules, different types of TDs, and different combinations

of deviation calculation components. So a large amount of improved PID controllers with different structures can be constructed. As long as there are reasonable transition process adjustment and differential signals, the effect of conventional PID controller can also be greatly improved even though linear combination shown in equation (7) is adopted. It should also be pointed out that the nonlinear combinations in equations (8)-(10) include many intelligent functions. Many learning experiences from engineering application can be easily achieved by nonlinear combination such as “determining the gain value according to the deviation.” Based on the above two facts, further study on special nonlinear control rules is full of practical significance.

2.1.4. Extended State Observer (ESO) and Disturbance Compensation. According to the study on estimation of performance assignment factor $a(t) = f(x_1(t), x_2(t), t)$, a second-order control object can be defined as follows:

$$\begin{cases} \dot{x}_1(t) = x_2(t), \\ \dot{x}_2(t) = f(x_1(t), x_2(t), \omega(t), t) + bu, \\ y = x_1(t), \end{cases} \quad (12)$$

where $\omega(t)$ is the external disturbance. The parameter, which can present the control process in equation (12), is shown as follows:

$$a(t) = f(x_1(t), x_2(t), \omega(t), t). \quad (13)$$

Then take equation (13) as an unknown extended state parameter:

$$x_3(t) = a(t). \quad (14)$$

So the system described in equation (12) is converted into a linear system:

$$\begin{cases} \dot{x}_1(t) = x_2(t), \\ \dot{x}_2(t) = x_3(t) + bu, \\ \dot{x}_3(t) = \omega_0(t), \\ y = x_1(t), \end{cases} \quad (15)$$

where $\omega_0(t)$ is not exactly available. However, the nonlinear system is transformed into a linear system shown in equation (15). The state observer is established as follows:

$$\begin{cases} e = z_1 - y, \\ \dot{z}_1 = z_2 - \beta_{01}e, \\ \dot{z}_2 = z_3 - \beta_{02}e + bu, \\ \dot{z}_3 = -\beta_{03}e. \end{cases} \quad (16)$$

To further weaken the influence of $\omega_0(t)$ on system, the observer function in equation (15) is improved by a non-linear process:

$$\begin{cases} e = z_1 - y, \\ \dot{z}_1 = z_2 - \beta_{01}e, \\ \dot{z}_2 = z_3 - \beta_{02}\text{fal}\left(e, \frac{1}{2}, h\right) + bu, \\ \dot{z}_3 = -\beta_{03}\text{fal}\left(e, \frac{1}{4}, h\right). \end{cases} \quad (17)$$

After the improvement in equation (17), a better tracking performance of the state parameter $z_i(t)$ on $x_i(t)$ is achieved, and the application range is further extended. Observer in equations (16) and (17) mentioned above can be called ESO of the system in equation (12).

It should be noted that the essence of ESO $x_3(t) = a(t) = f(x_1(t), x_2(t), \omega(t), t)$ is the performance assignment factor $a(t) = f(x_1(t), x_2(t), \omega(t), t)$ referred above, which can be taken as the sum of all kinds of disturbances, namely, the total disturbance. By estimating the total disturbance of the system, the global control problem can be simplified as an error feedback issue referring to the proposed method in this paper. If $a(t) \equiv \text{const}$, the integral feedback $-k_0 \cdot e_0$ can be replaced by the estimation and

compensation processes, so the side effect of error integral feedback can be weakened.

2.2. Basic Structure of ADRC. The TD, ESO, and NLSEF are used to construct the ADRC which is suitable for complex controlled objects. Diagram is shown in Figure 9. The key ability of ESO is to observe the disturbance and then generate a correction based on the observed result. So ADRC can be generally concluded as a controller which can generate a correction automatically according to the observed disturbance. The TD, ESO, and NLSEF can be collocated and configured according to the characteristics of the controlled object. Therefore, hundreds of ADRCs can be designed for different systems with the same structure framework shown in Figure 9.

Taking a controlled object with second-order uncertainty as an example:

$$\begin{cases} \dot{x}_1 = x_2, \\ \dot{x}_2 = f(x_1, x_2, \omega(t), t) + bu, \\ y = x_1, \end{cases} \quad (18)$$

where $f(x_1, x_2, \omega(t), t)$ is unknown. The control algorithm of the ADRC is shown as follows:

$$\begin{cases} \text{arrange - transition - process} \begin{cases} \dot{v}_1 = v_2, \\ \dot{v}_2 = \text{fhan}(v_1 - v_1 v_2, r_0, h), \end{cases} \\ \\ \text{ESO} \begin{cases} e = z_1 - y, \\ fe_1 = \text{fal}(e, 0.5, h), \\ fe_2 = \text{fal}(e, 0.25, h), \\ \dot{z}_1 = (z_2 - \beta_{01}e), \\ \dot{z}_2 = (z_3 - \beta_{02}fe_1 + b_0u), \\ \dot{z}_3 = (-\beta_{03}fe_2), \end{cases} \\ \\ \text{NLSEF} \begin{cases} e_1 = v_1 - z_1, \\ e_2 = v_2 - z_2, \\ u_0 = \text{fhan}(e_1, ce_2, r, h_1), \end{cases} \\ \\ \text{disturbance - compensation} - u = \frac{(u_0 - z_3)}{b_0}, \end{cases} \quad (19)$$

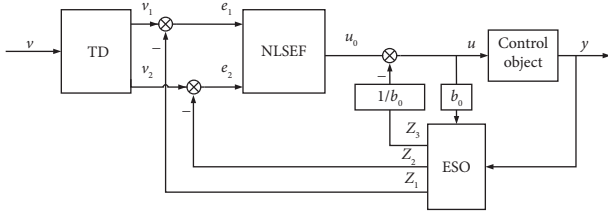


FIGURE 9: Principle diagram of the ADRC controller.

where r_0 , β_{01} , β_{02} , β_{03} , r , c , h_1 , and b_0 are the controller parameters. r_0 is decided by the requirement of the response speed and time. β_{01} , β_{02} , and β_{03} are only decided by signal sampling period without considering the controlled object. So only the damping factor c , gain r , precision factor h_1 , and compensation factor b_0 are needed to be adjusted in the controller. As to general systems, a relative high r is enough, and further increase in r has little effect on the control performance. Thus the remaining parameters h_1 , b_0 , and c similar to K_p , K_i , and K_d in PID controller are needed to be

adjusted, where l/h_1 , b_0 , and c , respectively, resembles K_p , K_i , and K_d .

2.3. ADRC Design for the Diesel Engine. The ADRC is composed of TD, ESO, and NLSEF. Such constructed ADRC can adapt to the strong nonlinearity and complex working environment of diesel engine. According to the characteristics of diesel engine, the modules of ADRC are designed as follows:

(1) TD design:

$$\begin{cases} v_1(k+1) = v_1(k) + hv_2(k), \\ v_1(k+1) = v_2(k) + hfst(v_1(k) - v_0, v_2(k), r, h_0), \end{cases} \quad (20)$$

where v_0 is the setting value.

(2) Estimation of the state and total disturbance (equation for ESO):

$$\begin{cases} \varepsilon_1 = z_1(k) - y(k), \\ z_1(k+1) = z_1(k) + h(z_2(k) - \beta_{01}\varepsilon_1), \\ z_2(k+1) = z_2(k) + h(z_3(k) - \beta_{02}fal(\varepsilon_1, \alpha_{01}, \delta) + bu(k)), \\ z_3(k+1) = z_3(k) - h\beta_{03}fal(\varepsilon_1, \alpha_{01}, \delta), \end{cases} \quad (21)$$

(3) formation of the control parameters:

$$\begin{cases} e_1 = v_1(k) - z_1(k), \\ e_2 = v_2(k) - z_2(k), \\ u_0 = \beta_{01}fal(e_1, \alpha_1, \delta) + \beta_{01}fal(e_1, \alpha_2, \delta), \\ u(k) = u_0 - \frac{z_3(k)}{b}, \end{cases} \quad (22)$$

$$\text{where } fal(\varepsilon, \alpha, \delta) = \begin{cases} |\varepsilon|^\alpha \text{sgn}(\varepsilon), & |\varepsilon| > \delta, \\ \varepsilon/\delta^{1-\alpha}, & |\varepsilon| \leq \delta. \end{cases}$$

The designed ADRC only requires the input $u(k)$ and output $y(k)$ of the system. The ADRC regards the external unknown factors (load, environment, etc.) and internal disturbances (engine cylinder heterogeneity, friction, etc.) of the controlled object (diesel engine) as the “total disturbance” of the system and then it estimates and corrects them by using the special ability of dealing with nonlinear problem. This control method has many advantages: (1) Adjusting the transition process by TD can effectively solve the contradiction between rapidity and overshoot. And the static error can be eliminated without using the integral process, which avoids side effects of the integral process. (2) The control problems of deterministic system and uncertain system are solved together. Also, the problem of “robustness” can be avoided effectively. (3) It does not depend on the accurate mathematical model and

the front data of the controlled object. (4) The ADRC has good control effect for time-delay system. According to the basic modules mentioned above, the ADRC is designed for the speed control system of the diesel engine. Figure 10 exhibits the structure diagram of the designed ADRC.

2.4. Engine Model Establishment. The established controlled engine model is mainly composed of four parts: cylinder charge efficiency submodel, engine intake submodel, thermal efficiency submodel, and engine power output submodel. The cylinder charge efficiency can be regarded as a function of engine speed according to the engine experimental data. Coefficient of the residual gas is ignored in the engine intake flow simulation model. The air flow rate of the diesel engine is calculated according to

$$\begin{aligned} q_{ma} &= \frac{\eta_v P_3 V n}{120} \\ &= \frac{\eta_v P_3 V n}{120 R_g T_3}, \end{aligned} \quad (23)$$

where η_v means the cylinder charge efficiency, P_3 means the intake pressure, V means the total cylinder volume, n means the engine speed, T_3 means the engine intake temperature, and R_g means the ideal gas constant.

The indicated thermal efficiency is a function of engine speed and air-fuel ratio, and the effect of air-fuel ratio on thermal efficiency is far more evident than engine speed. So

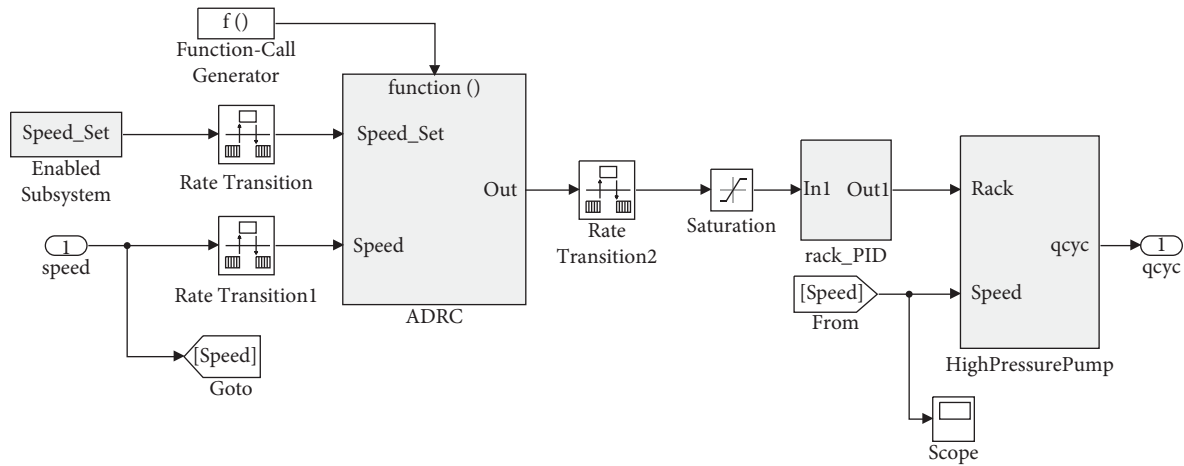


FIGURE 12: ADRC model for the engine speed control system.

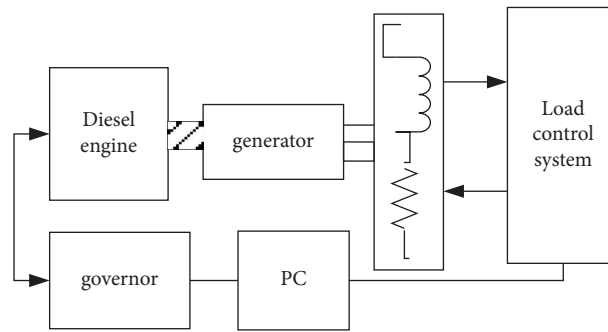


FIGURE 13: Diagram of the diesel engine speed control system.

3. Engine Experimental Bench

The engine experimental bench includes the diesel engine, FZC3000-225KVA load control system, PC with DS1103 single board computer, electronic governor, and hardware drive circuit board. The schematic diagram of the speed control system is shown in Figure 13, and the main parameters of the diesel engine are shown in Table 1. The load control system is used to control the load change of the engine to verify the control performance of the designed controllers under actual steady and transient conditions. The DS1103 single board computer, as the controller of the engine experimental bench, can compile and execute the designed control algorithm and strategy model. The hardware drive circuit board is used to perform the control signal output by the control algorithm to complete the speed control experiments. During the experiments, a ControlDesk is used to establish a monitoring interface to monitor and calibrate the relevant control parameters. The basic control strategy of speed control system is to automatically adjust the fuel supply according to the external load of the diesel engine, so as to control the speed in a certain range. An electronic governor with electromagnetic actuator is adopted to control fuel quantity of the diesel engine. The electromagnetic actuator is driven by PWM signal, and its actual displacement is obtained by using a displacement sensor.

To validate the control performance of the designed ADRC, a series of speed control experiments are carried out. Transient speed fluctuation rate and speed recovery time are commonly used to evaluate the dynamic speed control performance, and steady-state speed fluctuation rate is used to evaluate the steady speed control performance. Table 2 lists the performance indexes of the secondary power station that the experimental results will refer to.

4. Results and Discussion

4.1. Simulation Model Validation. To evaluate the reliability of the model, simulations are carried out for the speed change process during engine start-up with the main engine parameters in Table 1 and the main parameters of the simulation model in Table 3. It can be seen from Figure 14 that the simulation results are highly consistent with the experimental results, and the average error 1.31% and maximal error 6.90% are both within limit, verifying the established simulation model.

To further verify the characteristics of the simulation model, validations with load sudden changes are carried out. Figure 15 shows the comparisons of the simulation and experimental results. Similar speed fluctuation patterns are found in both simulation and experimental

TABLE 1: Main parameters of the diesel engine.

Engine parameter	Value
Type	6-cylinder, 4-stroke, in-line and turbocharged
Piston stroke (mm)	135
Cylinder diameter (mm)	114
Rated speed (r/min)	1500
Rated power (kW)	116
Fire order	1-5-3-6-2-4
Combustion chamber shape	ω
Rated torque (N·m)	738

TABLE 2: Performance indexes of the secondary power station.

Performance index	Value
Steady-state speed fluctuation rate (%)	0.4
Transient speed fluctuation rate (%)	7
Speed recovery time (s)	3

TABLE 3: Main parameters of the simulation model.

Parameter	Value
Total displacement (L)	8.27
Engine compression ratio	11
Moment of inertia ($\text{kg}\cdot\text{m}^2$)	25
Fuel calorific value (kJ/kg)	41.52
Supercharger compression ratio	1.6
Intake pipe volume (L)	0.4355
Exhaust pipe volume (L)	0.5311
Initial temperature of intake pipe (K)	303
Initial temperature of exhaust pipe (K)	303
Inlet temperature of cooling water (K)	303
Ambient temperature (K)	297
Ambient pressure (MPa)	0.1
Average temperature of cylinder liner (K)	534
Average temperature of cylinder head (K)	559
Average temperature of piston (K)	596
Diameter of intake valve seat (mm)	56.15
Diameter of exhaust valve seat (mm)	48.11
Time step (ms)	0.2

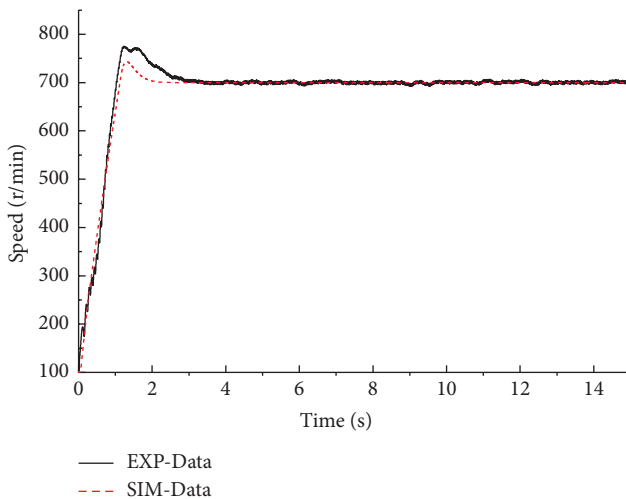


FIGURE 14: Simulation model verification during the engine start-up process.

results. However, the control-used model is a simplified mathematical description of the diesel engine, which leads to a higher model linearity than real diesel engine. This can explain the smaller transient speed fluctuation rate in simulation results. Overall, the mean value engine model is capable of validation for control performance after further optimization.

4.2. Simulation Result Analysis. Transient speed fluctuation rate is an important performance index of engine speed control. Load sudden change simulations are carried out to compare the control performance of the different control algorithms. A 100% load is loaded at the 40th second and unloaded at the 60th second in this paper. The traditional PID, improved PID, and ADRC are simulated to operate the model at the conditions of start-up, speed-up, load sudden change, and target speed sudden change with 100 r/min. The diesel engine model is sped up to 1500 r/min after a short period of idle speed operation and then followed with load sudden change experiments. Extracted differential signal is shown in Figure 16(a), and engine status parameter Z_3 is observed by the ESO in Figure 16(b). The target speed sudden increasing results are shown in Figure 17. The comparisons between the start-up and load sudden change simulation results of the proposed three kinds of control algorithms are shown in Figure 18. It is evident that the control performance of the TD-improved nonlinear PID is better than that of the traditional PID. The effect of differentiator is enhanced, reducing the maximum transient overshoot. Furthermore, the NLSEF achieved by fal (ϵ, α, δ) is capable of optimizing the control performance and adjusting the control effect according to the error value. The optimal control performance is achieved by the designed ADRC which is composed of TD, ESO, and NLSEF.

4.3. Experimental Result Analysis. Load sudden change experiments are carried out with the traditional PID, improved PID, and ADRC. Figures 19-21 show the load sudden change experimental results of the three control algorithms. Figure 22(a) and Figure 22(b), respectively, show the comparison results of the three control algorithms during sudden load process and sudden unload process. Table 4 exhibits the value comparisons. In this paper, differential signal extraction method is improved by TD in the ADRC. Because of the more reasonable differential signal extraction, the control performance for transient speed fluctuation rate and speed recovery time of the engine is significantly improved.

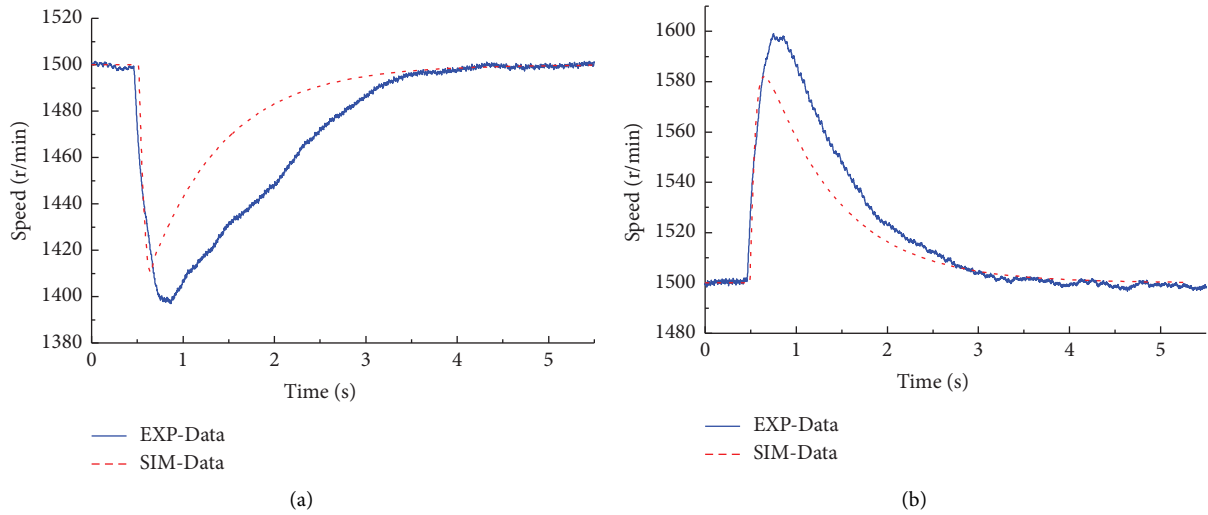


FIGURE 15: Simulation model verifications during the sudden load and sudden unload processes. (a) Sudden load process. (b) Sudden unload process.

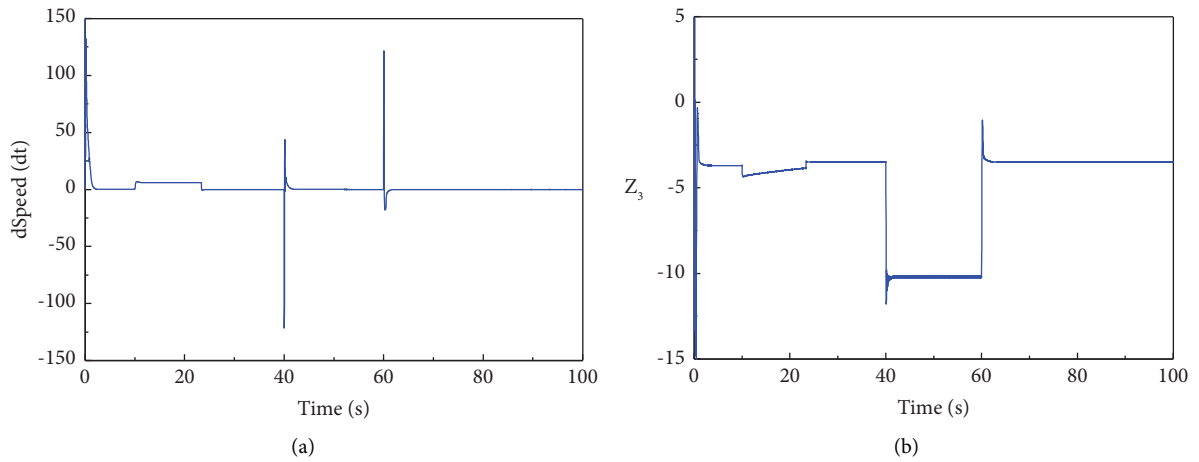


FIGURE 16: Speed differential signal and engine status parameter Z_3 . (a) Speed differential signal. (b) Engine status parameter Z_3 .

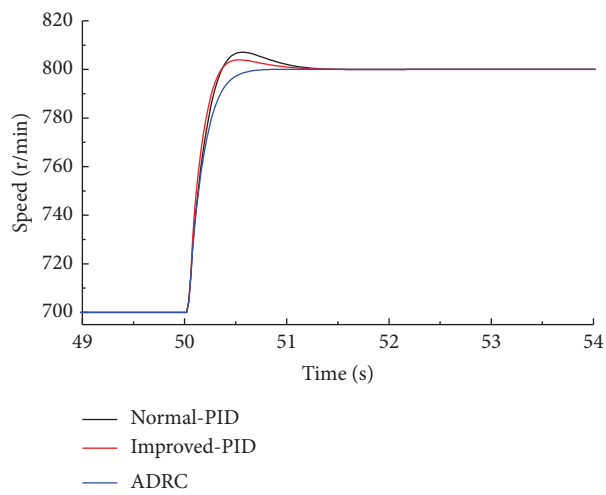


FIGURE 17: Target speed sudden increasing results with different control algorithms.

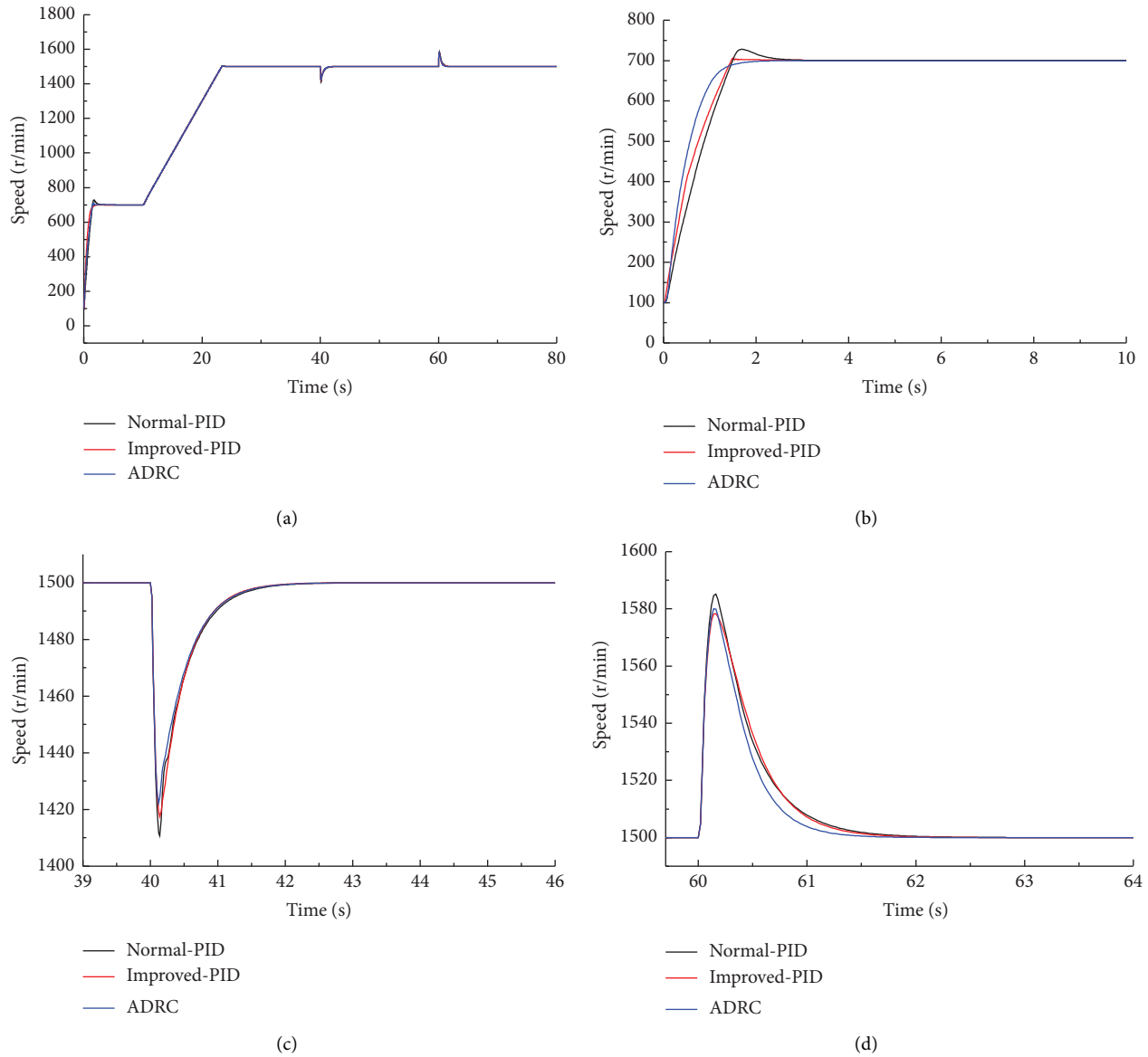


FIGURE 18: Simulation results of the speed control system with the three control algorithms. (a) The entire process of the engine speed variations. (b) The speed variations during engine start-up process. (c) The speed variations during sudden load process. (d) The speed variations during sudden unload process.

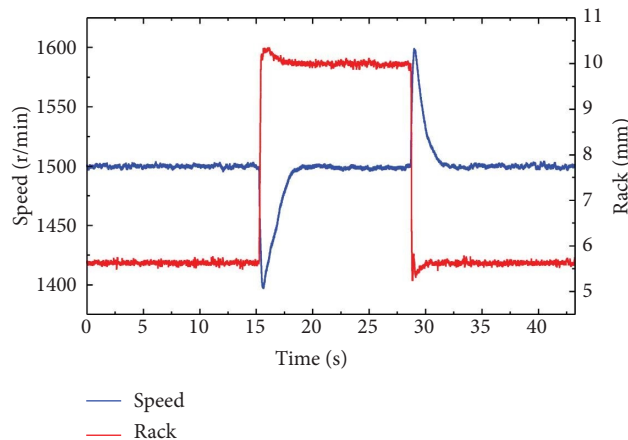


FIGURE 19: Experimental results of load sudden change for the traditional PID algorithm.

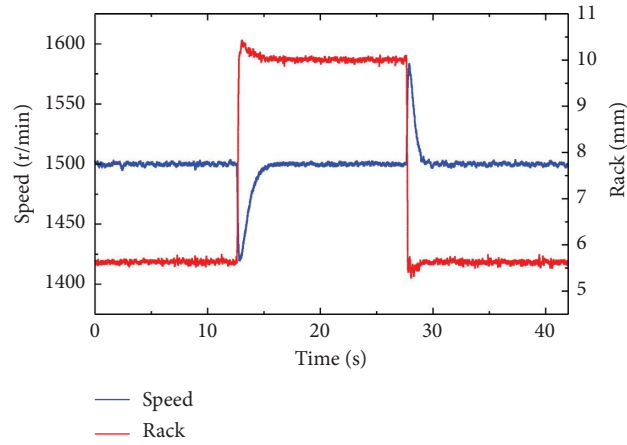


FIGURE 20: Experimental results of load sudden change for the improved PID algorithm.

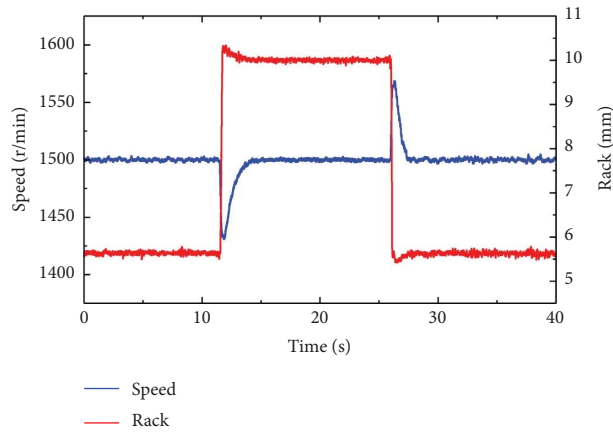


FIGURE 21: Experimental results of load sudden change for the ADRC algorithm.

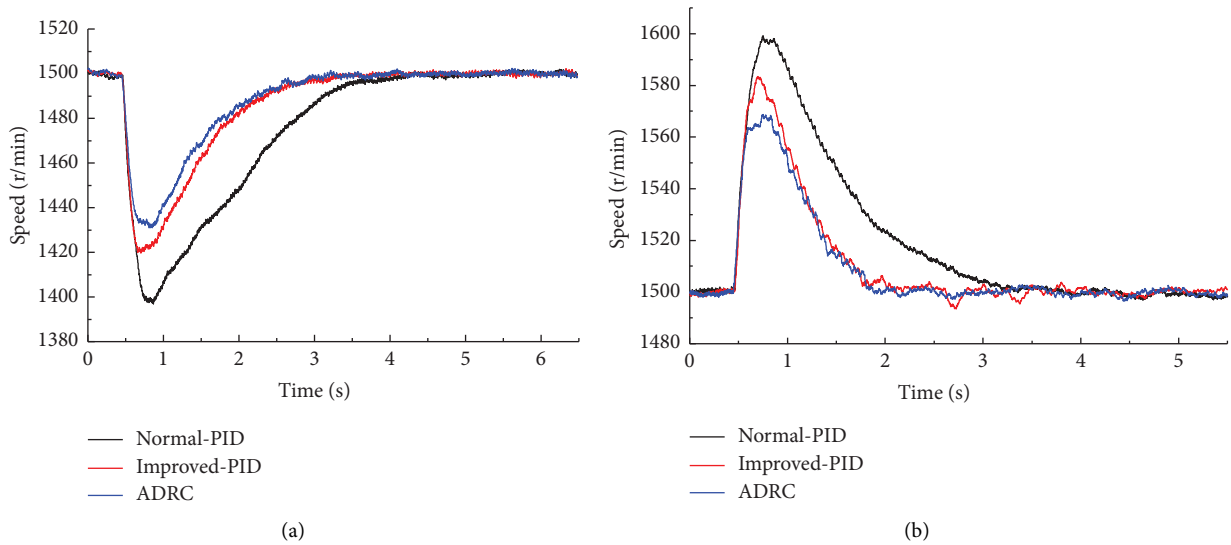


FIGURE 22: Comparisons of the experimental results for the three control algorithms (the target speed is the rated speed 1500 r/min). (a) Sudden load process. (b) Sudden unload process.

TABLE 4: Experimental data.

Controller type	Transient minimum speed for 100% sudden load (r/min)	Transient maximum speed for 100% sudden unload (r/min)	Transient speed fluctuation rate for 100% sudden load (%)	Transient speed fluctuation rate for 100% sudden unload (%)	Recovery time for sudden load (s)	Recovery time for sudden unload (s)	Steady-state speed fluctuation rate (%)
Traditional PID	1397	1599	6.87	6.60	2.96	2.71	0.249
Improved PID	1420	1583	5.33	5.53	2.55	1.57	0.235
ADRC	1432	1569	4.53	4.60	2.53	1.54	0.213

The ADRC control performance is presented by the blue line in Figure 22. The nonlinear combination rule adjusts the control parameters automatically according to the speed error and function f in equation (17). Z_3 , the output of ESO, is used to correct the control parameters. Z_3 is actually an observed value related to the engine speed, and it is a reflection of engine load. This is equivalent to a load feed forward added to the controller. According to the results in Table 4, compared with the traditional PID controller, the transient speed fluctuation rate of ADRC is, respectively, reduced by 34.06% and 30.30% and the recovery time of ADRC is, respectively, reduced by 14.53% and 43.17% under sudden load and sudden unload conditions. And the steady-state speed fluctuation rate is reduced by 14.46%.

5. Conclusions

In this paper, comprehensively considering the complex operating and environmental conditions, a new type of speed controller is designed with the active disturbance rejection control algorithm for the diesel engine. In addition, the structure of ADRC is designed by combining TD, ESO, and NLSEF to weaken the influence of simulation model and external disturbances. To verify the control performance of the designed ADRC, this paper establishes a control-used simulation model and builds an experimental bench. The results are as follows:

During the start-up process, the speed variations of the simulation model are compared with the experimental results. The simulation results are consistent with the experimental results, and the speed error is within the allowable range, which verifies the reliability of the simulation model. Compared with the simulation results of traditional PID and improved PID, the designed ADRC has the characteristics of faster response and smaller overshoot for the tracking of the target speed, which verifies the antidisturbance advantage of the proposed ADRC algorithm.

The load sudden change experiments are carried out on the engine experimental bench to verify the actual control performance of the designed ADRC. Compared with the traditional PID and improved PID, the performance indexes of the ADRC are significantly improved, which is consistent with the simulation results. The designed ADRC can take both steady and transient conditions of the engine into account and quickly and effectively weaken the influence of simulation model and external disturbances. This proves

that the designed ADRC is capable of improving the speed control performance of diesel engine.

Compared with the previous control strategy, ADRC has greater engineering application value in real-time control of diesel engine because it does not depend on accurate mathematical model of the controlled object. However, since the active disturbance rejection control algorithm can use different collocations and configurations for TD, ESO, and NLSEF to design the controller structure for the control system, the designed ADRC may not have the optimal structure. In the future research, we will conduct more in-depth research on structure optimization of ADRC for engine speed control systems.

Data Availability

All the data used to support the findings of the study are available within the article.

Conflicts of Interest

The authors declare that they have no known conflicts of interest.

Acknowledgments

This research was funded by the National Natural Science Foundation of China (51906225), the State Key Laboratory of Automotive Safety and Energy under Project KF2030, the Key Scientific Research Project of Colleges and Universities in Henan Province (20A470001), the Key R & D and Promotion Project in Henan Province (192102210225), and the 2022 Special Project of Professor Team to Help Enterprises Innovate and Drive Development (JSZLQY2022051).

References

- [1] A. Norouzi, H. Heidarifar, M. Shahbakhti, C. R. Koch, and H. Borhan, "Model predictive control of internal combustion engines: a review and future directions," *Energies*, vol. 14, no. 19, p. 6251, 2021.
- [2] W. Niklawy, M. Shahin, M. I. Amin, and A. Elmaihy, "Comprehensive analysis of combustion phasing of multi-injection HCCI diesel engine at different speeds and loads," *Fuel*, vol. 314, Article ID 123083, 2022.
- [3] Y. Yuan, M. Zhang, Y. Chen, and X. Mao, "Multi-sliding surface control for the speed regulation system of ship diesel engines," *Transactions of the Institute of Measurement and Control*, vol. 40, no. 1, pp. 22–34, 2018.

- [4] E. Kang, S. Hong, and M. Sunwoo, "Idle speed controller based on active disturbance rejection control in diesel engines," *International Journal of Automotive Technology*, vol. 17, no. 6, pp. 937–945, 2016.
- [5] T. A. Tran, "Analysis of the PID controller for marine diesel engine speed on simulink environment," in *Proceedings of the IEEE-2020 International Conference on Electrical Engineering and Control Technologies (CEEET)*, Melbourne, VIC, Australia, December 2020.
- [6] S. Banarezai and M. Shalchian, "Design of a model-based fuzzy-PID controller with self-tuning scaling factor for idle speed control of automotive engine," *Iranian Journal of Science and Technology, Transactions of Electrical Engineering*, vol. 43, no. 1, pp. 13–31, 2019.
- [7] G. F. Zhao, Y. Long, S. L. Ding, L. P. Yang, E. Z. Song, and X. Z. Ma, "Study of advanced control based on the RBF neural network theory in diesel engine speed control," *SAE International Journal of Engines*, vol. 13, no. 1, 2019.
- [8] K. Sandeep Rao, V. N. Siva Praneeth, and Y. V. Pavan Kumar, "Fuzzy logic-based intelligent PID controller for speed control of linear internal combustion engine," in *Innovations in Electrical and Electronic Engineering*, pp. 505–521, 2021.
- [9] T. Yang, Q. Cao, Q. Li, and H. Qiu, "A multi-directional multi-stable device: modeling, experiment verification and applications," *Mechanical Systems and Signal Processing*, vol. 146, Article ID 106986, 2021.
- [10] W. Z. Qiao and M. Mizumoto, "PID type fuzzy controller and parameters adaptive method," *Fuzzy Sets and Systems*, vol. 78, no. 1, pp. 23–35, 1996.
- [11] L. Cai, X. Mao, and Z. Ma, "Study on sliding mode variable structure control in nonlinear coupled systems of diesel engines," in *Proceedings of the 2018 10th International Conference on Computer and Automation Engineering*, pp. 205–210, Brisbane, Australia, February 2018.
- [12] Z. Ma, X. Mao, and L. Cai, "Research on the diesel engine with sliding mode variable structure theory," *Journal of Physics: Conference Series*, vol. 1016, Article ID 12017, 2018.
- [13] M. M. Abdo, A. R. Vali, A. R. Toloei, and M. R. Arvan, "Stabilization loop of a two axes gimbal system using self-tuning PID type fuzzy controller," *ISA Transactions*, vol. 53, no. 2, pp. 591–602, 2014.
- [14] P. B. Dickinson and A. T. Shenton, "A parameter space approach to constrained variance PID controller design," *Automatica*, vol. 45, no. 3, pp. 830–835, 2009.
- [15] Y. Xiong, S. Yang, W. Gou, H. Jiang, and K. Tan, "A fuzzy intelligent-integration PID idle control strategy for gas fueled SI engine," in *Proceedings of the 2013 International Conference on Computer Sciences and Applications*, pp. 357–360, Wuhan, China, December 2013.
- [16] R. Caponetto, L. Fortuna, S. Graziani, and M. G. Xibilia, "Genetic algorithms and applications in system engineering: a survey," *Transactions of the Institute of Measurement and Control*, vol. 15, no. 3, pp. 143–156, 1993.
- [17] R. A. Krohling and J. P. Rey, "Design of optimal disturbance rejection PID controllers using genetic algorithms," *IEEE Transactions on Evolutionary Computation*, vol. 5, no. 1, pp. 78–82, 2001.
- [18] M. W. Iruthayarajan and S. Baskar, "Evolutionary algorithms based design of multivariable PID controller," *Expert Systems with Applications*, vol. 36, no. 5, pp. 9159–9167, 2009.
- [19] J. Chen and T. C. Huang, "Applying neural networks to on-line updated PID controllers for nonlinear process control," *Journal of Process Control*, vol. 14, no. 2, pp. 211–230, 2004.
- [20] S. Jung and S. Kim, "Hardware implementation of a real-time neural network controller with a DSP and an FPGA for nonlinear systems," *IEEE Transactions on Industrial Electronics*, vol. 54, no. 1, pp. 265–271, 2007.
- [21] W. Meng and C. Guo, "Research on speed intelligent control based on neural networks for large marine main diesel engine," in *Proceedings of the 2010 8th World Congress on Intelligent Control and Automation*, pp. 4667–4670, Jinan, China, July 2010.
- [22] Y. W. Li, J. Z. Wu, and Y. B. Liu, "Feedforward compensation and PID neural network frequency control for internal-combustion Engine Generating Unit," *Transactions of CSICE*, vol. 25, no. 4, pp. 379–383, 2007.
- [23] X. Li, Y. Liu, H. Shu, R. Wang, Y. Yang, and C. Feng, "Disturbance observer-based discrete sliding-mode control for a marine diesel engine with variable sampling control technique," *Journal of Control Science and Engineering*, vol. 2020, Article ID 2456850, 17 pages, 2020.
- [24] J. Han, "The extended state observer of a class of uncertain systems," *Control and Decision*, vol. 10, no. 1, pp. 85–88, 1995.
- [25] T. Jiang, C. Huang, and L. Guo, "Control of uncertain nonlinear systems based on observers and estimators," *Automatica*, vol. 59, pp. 35–47, 2015.
- [26] S. Chen and F. Yan, "Decoupled, disturbance rejection control for a turbocharged diesel engine with dual-loop EGR system," *IFAC-PapersOnLine*, vol. 49, no. 11, pp. 619–624, 2016.
- [27] C. S. Tang and Y. H. Dai, "Novel active disturbance rejection control for permanent magnet linear synchronous motor without sensor," *Advanced Materials Research*, vol. 335-336, pp. 571–576, 2011.
- [28] G. Su, "Fuzzy ADRC controller design for PMSM speed regulation system," *Advanced Materials Research*, vol. 201-203, pp. 2405–2408, 2011.
- [29] Y. Shi and C. Hou, "Auto-disturbance-rejection controller design based on RBF neural networks," *Intelligent Control and Automation*, vol. 344, pp. 500–505, 2006.
- [30] X. L. Liu and L. P. Xiong, "Mechanical arm active disturbance rejection control based on artificial bee colony algorithm," *Applied Mechanics and Materials*, vol. 513-517, pp. 1511–1514, 2014.
- [31] J. Su, W. Qiu, H. Ma, and P. Y. Woo, "Calibration-free robotic eye-hand coordination based on an auto disturbance-rejection controller," *IEEE Transactions on Robotics*, vol. 20, no. 5, pp. 899–907, 2004.
- [32] H. B. Zhang, R. X. Wang, Y. H. Lin, and Y. J. Li, "Active disturbance rejection decoupling control for aero-engines," *Advanced Materials Research*, vol. 383-390, pp. 7702–7707, 2011.